

Subgap conductivity of a superconductor–normal-metal tunnel interface

F. W. J. Hekking and Yu.V. Nazarov*

Institut für Theoretische Festkörperphysik, Universität Karlsruhe Postfach 6980, 76128 Karlsruhe, Federal Republic of Germany

(Received 22 January 1993; revised manuscript received 23 April 1993)

At low temperatures, the transport through a superconductor–normal-metal tunnel interface is due to tunneling of electrons in pairs. We show that the rate for this process is often determined by the interference of the electron waves on a space scale determined by the coherence length. Therefore, the subgap current strongly depends on the layout of the electrodes within this space scale. The approach developed allows us to evaluate the subgap current for different layouts of interest.

It is well-known that the charge transport through a tunnel NS interface between a normal metal and a superconductor is strongly suppressed at voltages lower than Δ/e , Δ being the superconducting energy gap.¹ Indeed, energy conservation forbids the transfer of a normal electron with an energy below the gap to the superconductor, since it would have been converted into a quasiparticle with an energy larger than Δ .

Experimentally, some residual conductivity has been observed at subgap voltages even at very low temperatures. There is a tendency to ascribe this either to imperfections in the tunnel barrier or to normal inclusions in the superconductor. Another mechanism of the subgap conductivity is the so-called *two-electron tunneling*.² The point is that two normal electrons can be converted into a Cooper pair, and thus this transfer may cost no energy. The current will be proportional to the fourth power of tunnel matrix elements; therefore it is much smaller than the scale of the one-electron current above the gap.

The problem was previously treated under the simple assumption that the electron wave functions in both metals are just plane waves. In this case one can consider a barrier of arbitrary transparency in order to describe the crossover from a tunnel to a perfectly conducting interface³. But some important physics may be missed under this assumption. Let us compare the two realizations of the NS interface depicted in Fig. 1. In Fig. 1(a) the electron transmitted through the interface does not experience any scattering in the metals and never gets back to the junction. The plane-wave picture seems to be relevant for such a geometry. An alternative situation is shown in Fig. 1(b). This case is usually realized when the tunnel junction is formed by imposing two thin metal films. The transmitted electron gets back to the junction many times before leaving the junction region. Thus the tunneling occurs between electron states of very complex structure which emerges from interference between scattered waves.

One sees that at a NS interface two sources of coherence may interplay: the intrinsic coherence in the superconducting state, and the coherence on a mesoscopic length scale, leading to interference between electrons. This interference at a NS boundary has been the subject of recent experimental and theoretical work. Most of this

work concentrated on NS interfaces of high transparency, where the resistance R_T of the boundary was negligible, or at most comparable with the resistance R_N of the normal-metal side.^{4,5} The case of a barrier of arbitrary transparency has been discussed in Refs. 6,7.

In contrast to this, we will focus on the case of a tunnel NS interface, $R_N \ll R_T$, which is relevant from an experimental point of view.^{8,9} In this case, the subgap conductivity is much smaller than the normal-state conductivity, and is completely determined by the interference effects. Such a setup therefore allows one to reveal geometric effects on the subgap conductivity, which is a characteristic signature of interference. For a tunnel NS interface, the interference has no effect on one-electron transport, since the average one-electron density of states does not depend on the structure of the wave function. However, it matters for two-electron tunneling, since two electrons penetrating the barrier will interfere. This effect turns out to be drastic. The interference contribution will exceed the estimate made with the help of a plane-wave picture by many orders of magnitude.

Such an interference occurs at a space scale corresponding to the energy difference between the two elec-

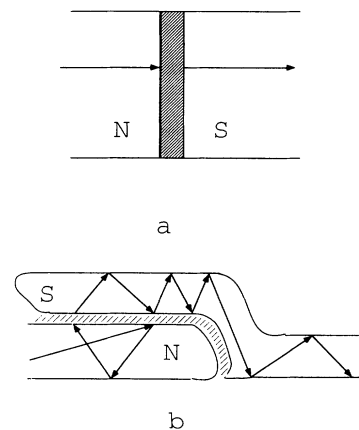


FIG. 1. Two typical realizations of a tunnel junction between a normal (N) and a superconducting (S) electrode. In (a) the electron moves ballistically, in (b) diffusively in the junction region.

tron states. It makes the probability of two-electron tunneling dependent on the system layout at the corresponding mesoscopic space scale. Our aim is to evaluate this interference effect for an arbitrary given layout. The rapid progress of nanotechnology makes it possible to fabricate numerous relevant structures, so it is worthwhile to be able to give guidelines to a designer. As we will see below, the subgap conductivity is strongly enhanced if the interference effect is essential.

We first review shortly the two-electron tunneling through a superconducting-normal interface as it has been discussed by Wilkins² and more recently by Hekking *et al.*¹⁰ The total Hamiltonian can be written as $\hat{H} = \hat{H}_N + \hat{H}_S + \hat{H}_T$. The subscripts N and S refer to the normal and the superconducting electrode respectively; the transfer of electrons through the tunnel interface is described by the tunnel Hamiltonian \hat{H}_T . The latter is expressed in terms of quasiparticle operators $\hat{\gamma}, \hat{\gamma}^\dagger$ for the superconductor, and electron operators \hat{a}, \hat{a}^\dagger for the normal metal:

$$\hat{H}_T = \sum_{\mathbf{k}, \mathbf{p}, \sigma} \{ t_{\mathbf{k}\mathbf{p}} \hat{a}_{\mathbf{k}, \sigma}^\dagger (u_{\mathbf{p}, \sigma} \hat{\gamma}_{\mathbf{p}, \sigma} + v_{\mathbf{p}, \sigma} \hat{\gamma}_{-\mathbf{p}, -\sigma}^\dagger) + t_{\mathbf{k}\mathbf{p}}^* (u_{\mathbf{p}, \sigma} \hat{\gamma}_{\mathbf{p}, \sigma}^\dagger + v_{\mathbf{p}, \sigma} \hat{\gamma}_{-\mathbf{p}, -\sigma}) \hat{a}_{\mathbf{k}, \sigma} \}. \quad (1)$$

Here, $t_{\mathbf{k}\mathbf{p}}$ are the tunnel matrix elements which we take to be spin independent, and $u_{\mathbf{p}, \sigma}, v_{\mathbf{p}, \sigma}$ are the BCS coherence factors;¹ the sum is taken over momenta \mathbf{k}, \mathbf{p} and spin $\sigma = \uparrow, \downarrow$.

Using second-order perturbation theory in \hat{H}_T one can calculate the amplitude for the transfer of two electrons from the normal to the superconducting electrode:

$$A_{\mathbf{k}\uparrow\mathbf{k}'\downarrow} = \sum_{\mathbf{p}} t_{\mathbf{k}\mathbf{p}}^* t_{\mathbf{k}'-\mathbf{p}}^* u_{\mathbf{p}} v_{\mathbf{p}} \left\{ \frac{1}{\xi_{\mathbf{k}} - \varepsilon_{\mathbf{p}}} + \frac{1}{\xi_{\mathbf{k}'} - \varepsilon_{\mathbf{p}}} \right\}. \quad (2)$$

Here the spin dependence of the coherence factors was dropped after using the relation $v_{\mathbf{p}, \uparrow} = -v_{-\mathbf{p}, \downarrow}$. We define electron energies $\xi_{\mathbf{k}}$ and $\zeta_{\mathbf{p}}$ for the normal and the superconducting electrode respectively, and quasiparticle energies $\varepsilon_{\mathbf{p}} = \sqrt{\Delta^2 + \zeta_{\mathbf{p}}^2}$. The denominators in (2) reflect the fact that a virtual state is formed when the first electron enters the superconductor as a quasiparticle. The second electron couples to this quasiparticle, thus forming a Cooper pair. The corresponding rate $\Gamma(V)$ as a function of the voltage V applied across the junction can be found by using Fermi's golden rule

$$\Gamma(V) = \frac{2\pi}{\hbar} \sum_{\mathbf{k}, \mathbf{k}'} |A_{\mathbf{k}\uparrow\mathbf{k}'\downarrow}|^2 f(\xi_{\mathbf{k}}) f(\xi_{\mathbf{k}'}) \delta(\xi_{\mathbf{k}} + \xi_{\mathbf{k}'} + 2eV). \quad (3)$$

It contains the Fermi functions f for electrons with energies $\xi_{\mathbf{k}}, \xi_{\mathbf{k}'}$ in the normal metal. We recall that the normal conductance of the junction is determined by the rate $\gamma(V)$ for the usual electron tunneling, which is proportional to $|t_{\mathbf{k}\mathbf{p}}|^2$: $\gamma(V) \propto \sum_{\mathbf{k}, \mathbf{p}} |t_{\mathbf{k}\mathbf{p}}|^2 f(\xi_{\mathbf{k}}) [1 - f_r(\zeta_{\mathbf{p}})] \delta(\xi_{\mathbf{k}} - \zeta_{\mathbf{p}} + eV)$.

The calculation of $|A_{\mathbf{k}\uparrow\mathbf{k}'\downarrow}|^2$ in Eq. (3) requires knowledge of the dependence of the $t_{\mathbf{k}\mathbf{p}}$ on the wave vectors \mathbf{k}

and \mathbf{p} . This dependence is strongly related to the nature of the electron motion in the electrodes, as we discussed above. Following Ref. 2 we assume first that plane electron waves propagating in the electrodes are transmitted specularly by a rectangular tunnel barrier with, say, a length L_b and a height U [See Fig. 1(a)]. The area of the junction will be denoted by S . If S is of the order of λ_F^2 (with λ_F the Fermi wavelength of the electrons) the components of momentum \mathbf{k}_{\parallel} and \mathbf{p}_{\parallel} parallel to the barrier plane are quantized, leading to discrete transport channels.¹¹ The corresponding quantum numbers left (l) and right (r) to the barrier, are equal for specular scattering: $n_l = n_r$. We define the effective number of channels $N_{\text{eff}} = G_T^2 R_Q / G_{\text{subgap}}$ contributing to the transport with G_T the normal-state conductance of the tunnel barrier, $R_Q = h/2e^2$ the quantum resistance, and G_{subgap} the subgap conductance due to two-electron tunneling. If the magnitude of $t_{\mathbf{k}\mathbf{p}}$ depends exponentially on energy, it is easy to show that $t_{\mathbf{k}\mathbf{p}} \propto \delta_{n_l, n_r} \exp -k_{\parallel}^2 \lambda^2$, with $\lambda^2 = \hbar L_b / \sqrt{8mU}$, where m is the electron mass. The calculation of the rate (3) can be performed using this model for $t_{\mathbf{k}\mathbf{p}}$, by averaging products of these matrix elements over directions of momentum. As a result we find $1/N_{\text{eff}}$ as the ratio

$$\frac{\Gamma}{\gamma^2} \propto \frac{\langle |t_{\mathbf{k}\mathbf{p}} t_{\mathbf{k}'\mathbf{p}}|_{\mathbf{p}}^2 \rangle_{\mathbf{k}\mathbf{k}'} / \langle |t_{\mathbf{k}\mathbf{p}}|^2 \rangle_{\mathbf{k}\mathbf{p}}^2}{= 4\pi\lambda^2/S} = 1/N_{\text{eff}}.$$

This result is obtained by assuming ballistic motion of the electrons in the electrodes. This assumption is correct only if the scattering of the electron is negligible. Scattering may occur at the boundaries of the electrodes or at impurities inside the electrodes. Both processes can be characterized by a space scale l_e , which corresponds to the distance the electron traverses before undergoing the first scattering event. Interference occurs on a space scale ξ_{cor} . The ballistic picture is valid if the typical size \sqrt{S} of the junction or ξ_{cor} is smaller than l_e . When these lengths are of the same order, we expect a crossover to different behavior. In the opposite limit the electron moves diffusively in the junction region. Due to interference between incoming and backscattered electron waves N_{eff} will decrease, thereby increasing the rate Γ , and hence the conductance due to two-electron tunneling.

Now we will present a method to describe two-electron tunneling in the diffusive transport regime, employing the quasiclassical approximation. This enables us to evaluate the tunnel matrix elements and express the rate Γ in terms of quasiclassical diffusion propagators. The method is similar to the one presented in Ref. 12. We start by rewriting the matrix elements $t_{\mathbf{k}\mathbf{p}} = \int dr dr' \psi_{\mathbf{k}}^*(r) \psi_{\mathbf{p}}(r') t(r, r')$, where $\psi_{\mathbf{p}}(r)$ forms a complete set of one-electron wave functions in the electrodes (although we still use indices k, p they no longer refer to plane waves), and $t(r, r')$ describes the tunneling from a point r' in the superconductor to a point r in the normal metal (primed space arguments refer to the superconductor). We also define a propagator from r_2 to r_1 by $K_{\xi}(r_1, r_2) = \sum_{\mathbf{k}} \delta(\xi - \xi_{\mathbf{k}}) \psi_{\mathbf{k}}(r_1) \psi_{\mathbf{k}}^*(r_2)$. With these definitions it is possible to rewrite Eq. (3) as

$$\Gamma(V) = \frac{2\pi}{\hbar} \int d\xi d\xi' d\zeta d\zeta' F(\zeta; \xi, \xi') F(\zeta'; \xi, \xi') \Xi(\zeta, \zeta'; \xi, \xi') f(\xi) f(\xi') \delta(\xi + \xi' + 2eV), \quad (4)$$

with $F(\zeta; \xi, \xi') = u(\zeta)v(\zeta)\{(\xi + eV - \varepsilon)^{-1} + (\xi' + eV - \varepsilon)^{-1}\}$ where $\varepsilon = \sqrt{\Delta^2 + \zeta^2}$, and

$$\Xi(\zeta, \zeta'; \xi, \xi') = \int d^3r_1 \dots d^3r_4 \int d^3r'_1 \dots d^3r'_4 t^*(r_1, r'_1) t^*(r_2, r'_2) t(r_3, r'_3) t(r_4, r'_4) K_\xi(r_1, r_3) K_{\xi'}(r_2, r_4) K_\zeta(r'_2, r'_1) K_{\zeta'}(r'_4, r'_3). \quad (5)$$

The physical meaning of Eq. (4) can be understood easily by depicting the integrand of Eq. (5) diagrammatically, as has been done in Fig. 2.¹³ We see two electrons that propagate in the normal electrode with energy ξ and ξ' . The first electron reaches the barrier at r_1 and tunnels to r'_1 , the second electron tunnels from r_2 to r'_2 ; both change their energy to ζ . Since tunneling occurs only between neighboring positions, we have in addition $r_i \approx r'_i$. The diagram expresses a probability, and therefore is completed by adding the time-reversed process.

To analyze expression (5), it is important to consider the scale of separation of the coordinates $r_1 \approx r'_1, \dots, r_4 \approx r'_4$ lying on the interface. In the ballistic transport regime, these coordinates are separated only by a few Fermi wavelengths. In this case the contribution depends on properties of the tunnel barrier only. Below we will concentrate on contributions to (5) which arise when the region of integration is defined by coordinates which are pairwise close, but with the pairs separated by a distance much larger than the Fermi wavelength. These contributions contain averaged products of two propagators K , which are known to decay on a mesoscopic scale in the diffusive transport regime.¹⁴ These products correspond to the semiclassical motion of electrons from one point on the interface back to another point on this interface. They describe the interference between scattered waves. In the diffusive regime these contributions dominate; that is why we concentrate on them.

There are three types of contributions, which are depicted in Fig 3. Figure 3(a) corresponds to the case $r_1 \approx r_2$ and $r_3 \approx r_4$. The interference contribution originates from the normal electrode. Figure 3(b) describes

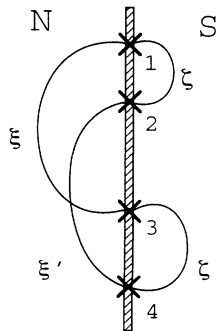


FIG. 2. Diagram corresponding to Eq. (5). Electrons propagate (solid lines) with energy ξ, ξ' in the normal (N) and energy ζ, ζ' in the superconducting (S) electrode. They tunnel through the barrier (shaded region) at positions 1, ..., 4, marked by crosses.

the opposite situation with interference occurring in the superconducting electrode. Here, $r_1 \approx r_3$ and $r_2 \approx r_4$. Finally, in Fig. 3(c), interference occurs both in the normal and in the superconducting electrode, when $r_1 \approx r_4$ and $r_2 \approx r_3$. Qualitatively, this diagram describes the correlation between *different* interference contributions in both electrodes, and thus should be small compared to the previous diagrams. Therefore, the total effect can be represented as the sum of the interference contributions from the superconducting and the normal metal.

As an example we will discuss the contribution of Fig. 3(b) to the rate (4) in some detail. The averaged product of the propagators in the superconductor determines the semiclassical conditional probability $P(r'_1, r'_2; n, n'; t)$ that an electron with position r'_2 and momentum direction n' at time $t = 0$ has position r'_1 and momentum direction n at time t . Since the tunnel amplitude $t(r, r')$ is nonzero only when r and r' are close to the junction interface, we can restrict spatial integrations to planar integrations over the junction surface. It is possible to show that¹²

$$\begin{aligned} \Xi_S = \Xi_S(\zeta - \zeta') &= \frac{\hbar}{8\pi^3 e^4 \nu_S} \int d^2r'_1 d^2r'_2 \\ &\times \int d^2n d^2n' g(n, r'_1) g(n', r'_2) \\ &\times \int dt e^{i(\zeta - \zeta')t/\hbar} P(r'_1, r'_2; n, n'; |t|) \end{aligned} \quad (6)$$

where ν_S is the density of states for the superconduc-

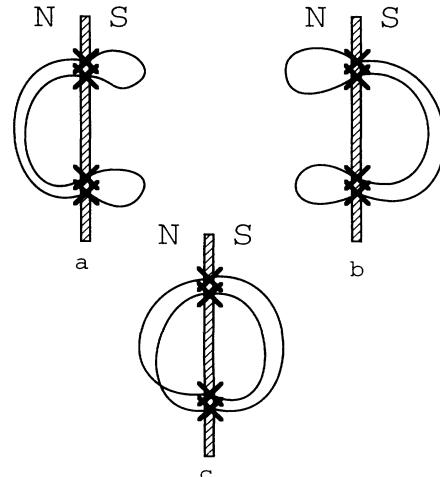


FIG. 3. Contributions to the subgap conductivity due to interference in (a) the normal electrode, (b) the superconducting electrode, and (c) both electrodes.

tor for two spin directions and $\int d^2n$ denotes integration over directions of momentum. The function $g(n, r)$ defines the normal conductance of the junction: $G_T = \int d^2r \int d^2n g(n, r)$. An expression similar to (6) can be obtained for Fig. 3(a), by replacing subscript $S \rightarrow N$, energies $\zeta \rightarrow \xi$, and primed space arguments by unprimed ones.

Let us start our consideration of concrete layouts with the simplest geometry of an infinite uniform junction between a normal and a superconducting film [Fig. 4(a)]. We assume that the film thickness is much less than the coherence length in the superconductor. Then we can exploit the picture of two-dimensional electron diffusion. The probability function we need is given by

$$P(r_1, r_2; t) = \frac{1}{4\pi D t d} \exp(-|r_1 - r_2|^2/4Dt), \quad (7)$$

d being the thickness of either the superconducting or the normal-metal film. Taking the Fourier transform of this function with respect to time and integrating (6) over coordinates we obtain

$$\Xi_S(\zeta - \zeta') = \frac{G_T^2}{4\pi^2 e^4 S \nu_S d_S} \delta(\zeta - \zeta'); \quad (8)$$

$$\Xi_N(\xi - \xi') = \frac{G_T^2}{4\pi^2 e^4 S \nu_N d_N} \delta(\xi - \xi');$$

The current is given by a sum of two terms ($eV \lesssim \Delta \gg T$):

$$\begin{aligned} I(V) &= I_N + I_S; \\ I_N &= \frac{G_T^2 \hbar}{e^3 S \nu_N d_N}; \\ I_S &= \frac{G_T^2 \hbar}{e^3 S \nu_S d_S} \frac{eV}{2\pi\Delta\sqrt{1 - eV/\Delta}}. \end{aligned} \quad (9)$$

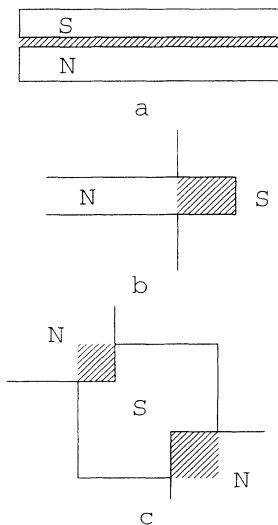


FIG. 4. Various layouts discussed in the text: (a) infinite uniform junction, (b) normal electrode connected to a superconducting half plane, and (c) a superconducting island connected to two normal electrodes.

It is plotted in Fig. 5. The part emerging from the interference in the normal metal does not depend on voltage. So the current sharply jumps at zero voltage, provided $T = 0$. The jump is smoothed at voltages of the order of the temperature:

$$I(V, T) = I_N \tanh(eV/2T). \quad (10)$$

The other contribution diverges near the threshold voltage indicating the necessity to make use of higher-order terms in tunneling amplitudes to describe the crossover between two-electron and one-electron tunneling.

It is worthwhile to compare the magnitude of the result with the one we derived assuming ballistic motion. The order of the ratio at voltages of the order of Δ is $I_{\text{interference}}/I_{\text{ballistic}} \simeq \xi_{\text{clean}}/d$, ξ_{clean} being the coherence length in the pure superconductor. Therefore the interference term dominates under the assumptions we made.

The coherence of two electrons moving along a normal or superconducting film decays on a scale given by the coherence length $\xi_{\text{cor}}^{N,S} = \sqrt{D/\max\{eV, T\}}$, $\sqrt{D/\Delta}$, respectively. The relations (10) are valid, provided the junction size is much larger than these lengths. In the opposite limit of small junctions, the subgap conductivity will be determined by the junction surroundings, rather than by the junction itself. Let us illustrate this by considering the geometry in Fig. 4(b), where a normal electrode is connected to a superconducting sheet by the tunnel junction. In this case we find

$$\begin{aligned} \Xi_S(\zeta - \zeta') &= \frac{\hbar R_{\square}^S G_T^2}{e^2 8\pi^4} \ln \frac{\hbar}{(\zeta - \zeta')\tau}; \\ \Xi_N(\xi - \xi') &= \frac{\hbar R_{\square}^N G_T^2}{e^2 8\pi^4} \ln \frac{\hbar}{(\xi - \xi')\tau}. \end{aligned} \quad (11)$$

The time τ is of the order of S/D , the time spent in the junction area, and provides a lower cutoff for the Fourier integral. The sheet resistance of the normal (supercon-

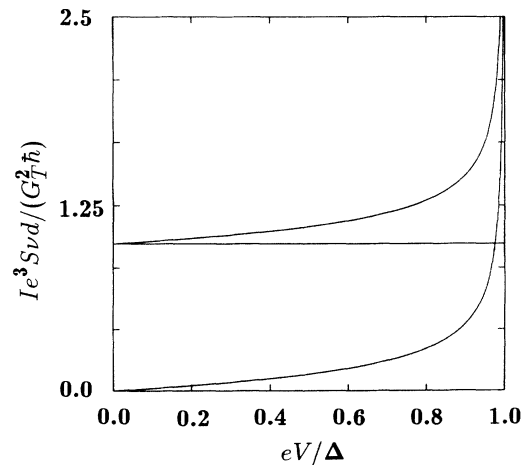


FIG. 5. $I - V$ characteristics for an infinite junction. The curves (from bottom to top) represent I_S , I_N , and $I(V) = I_S + I_N$.

ducting) film is given by $R_{\square}^{N(S)} = (e^2 \nu D_{N(S)} d_{N(S)})^{-1}$. Indeed, the result not only depends on the properties of the tunnel barrier itself (through the dependence on G_T), but also on properties of its surroundings through the dependence on R_{\square} . Moreover, the dependence on the precise geometry of the layout enters through numerical prefactors. If, e.g., the tunneling would occur towards an infinite superconducting sheet instead of a superconducting half plane, the semiclassical probability P would be twice smaller, thus decreasing Ξ , and hence the rate Γ , by a factor of 2. The current is again given by a sum of two terms I_N and I_S :

$$I_N = \frac{V}{\pi} R_{\square, N} G_T^2 \ln \frac{\hbar}{eV\tau}; \quad I_S = \frac{V}{\pi} R_{\square, S} G_T^2 \ln \frac{\hbar}{\Delta\tau}. \quad (12)$$

Note that, in contrast to Eq. (10), the subgap conductivity depends only weakly on the junction area through the cutoff time τ .

We finally consider the geometry depicted in Fig. 4(c). It consists of a small island (length L_S , thickness d_S), coupled to two macroscopic leads by tunnel barriers. The grain is linked capacitively to the leads. Electron transport through such a system, characterized by a small electric capacitance C , has been studied both experimentally and theoretically in great detail during the past years.¹⁵ The key point is that variations of the charge of the island in the course of electron tunneling increase the electrostatic energy, typically by an amount $E_C = e^2/2C$. This is why electron tunneling through a small grain is suppressed (Coulomb blockade). The case of a superconducting island connected to two normal electrodes (NSN geometry), was studied recently in Refs. 9,10,16. Our method to include interference effects can also be applied to this case. The charging energy E_C will enter our results explicitly via the virtual state denominators in (2),¹⁰ resulting in a dependence of the function F on E_C . We will restrict ourselves to the situation in which E_C is smaller than the superconducting gap: $E_C < \Delta$. In order to calculate the contribution due to interference on the island we assume that the time $\hbar/(\Delta - E_C)$ spent by the virtual electron on the island is much longer than than the classical diffusion time L_S^2/D . In this case, the electron motion covers the whole island and the probability P is constant: $P = 1/(L_S^2 d_S)$. As a result we

find:

$$\Xi_S(\zeta - \zeta') = \frac{\hbar^2 w_S G_T^2}{4\pi^2 e^4} \delta(\zeta - \zeta') \quad (13)$$

where $w_S = 1/(\nu_S L_S^2 d_S)$ denotes the level spacing of the island, which shows once more that the rate (4) is not only determined by properties of the tunnel barrier. The corresponding current I_S reads

$$I_S = V \frac{2\hbar}{\pi e^2} G_T^2 \frac{w_S \Delta}{E_C^2} \left[\frac{\pi}{2} - \frac{2\Delta}{\sqrt{\Delta^2 - E_C^2}} \left\{ 1 - \frac{E_C^2}{\Delta^2 - E_C^2} \right\} \right] \\ \times \arctan \sqrt{\frac{\Delta - E_C}{\Delta + E_C} + \frac{\Delta E_C}{\Delta^2 - E_C^2}}. \quad (14)$$

When interference in the normal electrode is taken into account, we find

$$\Xi_N(\xi - \xi') = (\hbar/e^2) (R_{\square}^N G_T^2 / 4\pi^4) \ln[\hbar/(\xi - \xi')\tau], \quad (15)$$

as in Eq. (11), but larger by a factor of 2, due to the difference in geometry. The resulting current reads:

$$I_N = \frac{2V}{\pi^3} R_{\square}^N G_T^2 \ln \frac{\hbar}{eV\tau} \left\{ \frac{4\Delta}{\sqrt{\Delta^2 - E_C^2}} \right. \\ \left. \times \arctan \sqrt{\frac{\Delta + E_C}{\Delta - E_C}} \right\}^2. \quad (16)$$

In conclusion, we evaluated the low-voltage subgap conductivity of a NS boundary interface. The main transport mechanism under subgap conditions is two-electron tunneling, as the transfer of single electrons is strongly suppressed. Due to the possibility of interference between the two electrons, the subgap conductance is determined by the conditions of electron motion on a space scale given by the coherence length. Therefore it depends on the system layout on a mesoscopic scale. We presented an approach which gives exact results for any layout given. It is found that the effect is drastic: The actual subgap current exceeds the result obtained when interference is neglected by several orders of magnitude.

The authors are grateful to M. Devoret, D. Esteve, J. Mooij, A. Schmid, and G. Schön for a set of valuable discussions. This work was supported in part by Sonderforschungsbereich of the Deutsche Forschungsgemeinschaft.

* Present address: Department of Applied Physics, Delft University of Technology, Lorentzweg 1, Postbus 5046, 2600 GA Delft, the Netherlands.

¹ M. Tinkham, *Introduction to Superconductivity* (McGraw-Hill, New York, 1975).

² J. W. Wilkins, in *Tunneling Phenomena in Solids*, edited by E. Burstein and S. Lundqvist (Plenum, New York, 1969), p. 333.

³ G. E. Blonder, M. Tinkham, and T. M. Klapwijk, *Phys. Rev. B* **25**, 4515 (1982).

⁴ A. Kastalsky, A. W. Kleinsasser, L. H. Greene, R. Bhat, F. P. Milliken, and J. P. Harbison, *Phys. Rev. Lett.* **67**, 3026

(1991).

⁵ B. J. van Wees, P. de Vries, P. Magnée, and T. M. Klapwijk, *Phys. Rev. Lett.* **69**, 510 (1992).

⁶ C. W. J. Beenakker, *Phys. Rev. B* **46**, 12841 (1992).

⁷ A. F. Volkov, *Pis'ma Zh. Eksp. Teor. Fiz.* **55**, 713 (1992) [*JETP Lett.* **55**, 745 (1992)].

⁸ M. T. Tuominen, J. M. Hergenrother, T. S. Tighe, and M. Tinkham, *Phys. Rev. Lett.* **69**, 1997 (1992).

⁹ T. M. Eiles, J. M. Martinis, and M. H. Devoret, *Phys. Rev. Lett.* **70**, 1863 (1993).

¹⁰ F. W. J. Hekking, L. I. Glazman, K. A. Matveev, and R. I. Shekter, *Phys. Rev. Lett.* **70**, 4138 (1993).

- ¹¹ Y. Imry, in *Directions in Condensed Matter Physics*, edited by G. Grinstein and G. Mazenko (World Scientific, Singapore, 1986), p. 100.
- ¹² D. V. Averin and Yu. V. Nazarov, *Phys. Rev. Lett.* **65**, 2446 (1990); in *Single Charge Tunneling*, edited by H. Grabert and M. H. Devoret (Plenum, New York, 1992), Chap. 6.3.
- ¹³ See F. Guinea and G. Schön, *Physica B* **152**, 165 (1988). In this paper, similar diagrams for the subgap conductance of a NS junction have been studied in the context of an imaginary-time analysis. The main point in the present paper, however, is the dependence of these diagrams on the geometry under consideration.
- ¹⁴ B. L. Al'tshuler and A. G. Aronov, in *Electron-Electron Interactions in Disordered Systems: Modern Problems in Condensed Matter Sciences*, edited by A. L. Efros and M. Pollak (North-Holland, Amsterdam, 1985), p. 21.
- ¹⁵ D. V. Averin and K. K. Likharev, in *Mesoscopic Phenomena in Solids*, edited by B. L. Altshuler *et al.* (Elsevier, Amsterdam, 1991), p. 173; *Single Charge Tunneling*, edited by H. Grabert and M. H. Devoret (Plenum, New York, 1992).
- ¹⁶ J. M. Hergenrother, M. T. Tuominen, and M. Tinkham (unpublished).